ACS OMEGA

http://pubs.acs.org/journal/acsodf

Article

Isomers of the Allyl Carbocation $C_3H_5^+$ in Solid Salts: Infrared Spectra and Structures

Evgenii S. Stoyanov,* Irina Yu. Bagryanskaya, and Irina V. Stoyanova

Cite This: *ACS Omega* 2021, 6, 23691−23699

Read Online

ACCESS | Metrics & More | Article Recommendations | Supporting Information

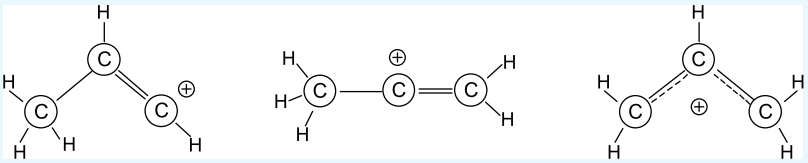

ABSTRACT: Three isomers of the allyl cation $C_3H_5^+$ were obtained in salts with the carborane anion $CHB_{11}Cl_{11}^-$. Two of them, angular $CH_3{-}CH{=}CH^+$ (**I**) and linear $CH_3{-}C^+{=}CH_2$ (**II**), were characterized by X-ray crystallography, and the third one, $(CH_2CHCH_2)^+$ (**III**), is formed in an amorphous salt. The stretch vibration of the charged double bond $C{=}C^+$ of **I** and **II** is decreased by 162 cm^{-1} (**I**) or 76 cm^{-1} (**II**) as compared to that of neutral propene. This result contradicts the prediction of DFT and MP2 calculations with the 6-311G++(d,p) basis set that the appearance of the positive charge on the C=C bond should increase its stretch vibration by 200 cm^{-1} (**I**) or 210 cm^{-1} (**II**). According to infrared spectra, the CC bonds in isomer **III** have one-and-a-half bond status. Isomers **I** and **II** in the crystal lattice are stabilized due to uniform ionic interactions with neighboring anions with partial transfer of a positive charge to them. Additional stabilization of **II** is provided by a weak hyperconjugation effect. Isomer **III** is stabilized in the amorphous phase due to ion paring with a counterion and a strong intramolecular hyperconjugation effect.

1. INTRODUCTION

Considerable progress has been achieved in the research on saturated and aromatic carbocations.[1−3] The same cannot be said about unsaturated alkene cations. Despite extensive theoretical and experimental research in the past five decades,[4−12] our knowledge about the simplest alkene carbocations not stabilized by heteroatoms and aromatic groups remains limited. It derives mainly from theoretical research and a moderate number of experimental studies. For instance, the simplest vinyl cation $C_2H_3^+$ and isomers of cations $C_3H_3^+$ and $C_3H_5^+$ have been studied experimentally in vacuum by mass-selected IR spectroscopy.[13−15] In a solid phase, not stabilized alkene carbocations are isolated without a counterion in a cryogenic Ar matrix[16] or superacidic SbF_5 matrix.[17] It looks like these cations cannot be stable under ambient conditions. Nonetheless, the isobutylene$^+$ carbocation obtained as a carborane salt and characterized by IR spectroscopy and X-ray crystallography appears to be stable up to 100 °C. It has specific IR spectroscopic properties.[18]

From studies on solvolysis reactions, it has been concluded that vinyl- or allyl-type carbocations are highly reactive and therefore difficult to study.[5,7,10] On the other hand, Mayr and co-workers have shown that their expected reactivity is exaggerated.[19] Recently, the high reactivity of the benzyl carbocation was explained: when acting as a strong protonating agent, it converts into a carbene molecule, whose high reactivity can be perceived as the reactivity of the carbocation.[20] Thus, the latest research revealed unexpected properties of unsaturated alkene carbocations.

In this work, we studied isomers of the allyl carbocation $C_3H_5^+$ in amorphous and crystalline phases at room temperature by IR spectroscopy and X-ray crystallography. As a counterion, the undecachlorocarborane anion $CHB_{11}Cl_{11}^-$ was chosen. Its extreme stability and low basicity promote the formation of stable salts with highly reactive cations.[21]

2. RESULTS

Injection of gaseous 1,2-dichloropropane (hereinafter abbreviated as DCP) into an IR cell-reactor with a thin layer of $H(CHB_{11}Cl_{11}^-)$ (hereafter abbreviated as $H\{Cl_{11}\}$) covering the Si windows leads to a surface reaction with a release of HCl. It was found that the molar ratio of the formed HCl to the reacted acid is close to 2 (see the Experimental Section), that is, the overall reaction proceeds according to eq 1

$$C_3H_6Cl_2 + H\{Cl_{11}\} \rightarrow C_3H_5^+\{Cl_{11}^-\} + 2HCl \quad (1)$$

It is a two-step reaction: First, the unstable cation $C_3H_6Cl^+$ is formed, which rapidly decomposes to $C_3H_5^+$ + HCl, similar to the reaction of dichlorobutane with $H\{Cl_{11}\}$, forming the butene cation, $C_4H_7^+$.[18] In the course of reaction 1, absorption

Received: March 11, 2021
Accepted: August 13, 2021
Published: September 8, 2021

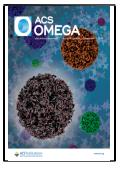

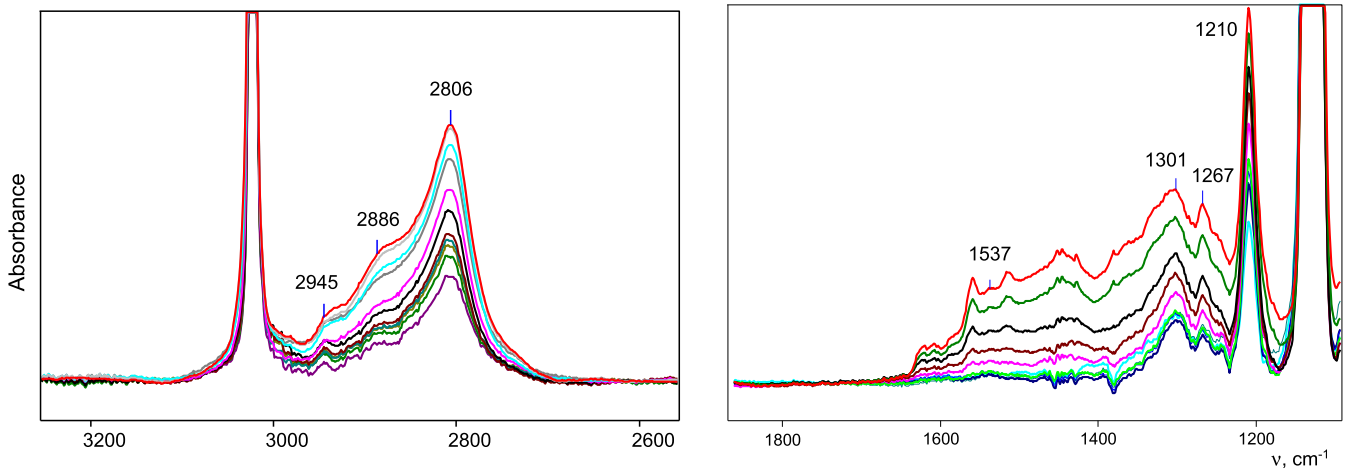

Figure 1. IR spectra of carbocations produced by the interaction of DCP with $H\{Cl_{11}\}$ until complete consumption of the free acid (red spectrum). The spectra of gaseous HCl and DCP and those of the free acid are compensated.

intensity of the free acid decreased, and when it approached zero, the reaction was stopped by removing the gas phase in vacuum. The spectra of the products formed by the reaction were isolated from the recorded spectrum by successive subtraction of the spectra of DCP vapors, gaseous HCl, and unreacted acid. They showed (Figure 1) that the carbocation $C_3H_5^+$ with the most characteristic frequencies at 2806, 1301, 1267, and 1210 cm^{-1} forms first. Then, the formation of the second carbocation begins with a broad intense absorption pattern in the range of 1200−1600 cm^{-1}. It will be shown below that this is the product of the interaction of $C_3H_5^+$ with DCP.

Repetition of this experiment with a thinner layer of the sublimated acid leads to faster completion of the reaction (the $H\{Cl_{11}\}$ acid is polymeric,[22] which slows down its interaction with bases) with the formation of the first cation less contaminated by the second (Figure 2).

The purest salt of the $C_3H_5^+$ cation is obtained through the interaction of DCP with monomeric molecules of the $CH_2Cl^+\{Cl_{11}^-\}$ salt via eq 2.

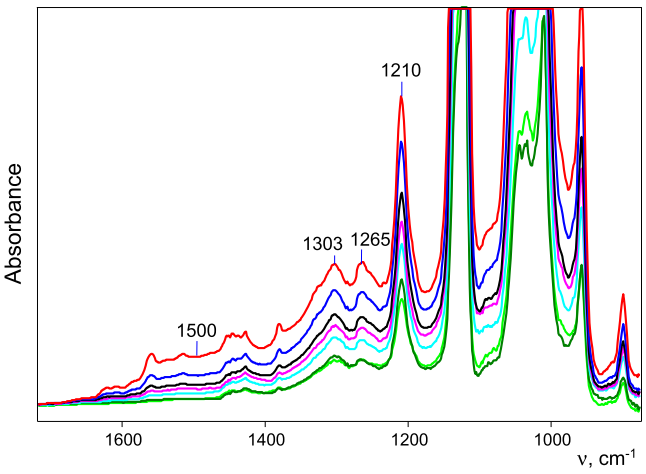

Figure 2. IR spectra of carbocations formed during the interaction of DCP with a thinner $H\{Cl_{11}\}$ layer than in the experiment shown in Figure 1. Spectra of the free acid, DCP vapors, and HCl are compensated. The red spectrum corresponds to complete consumption of the acid.

$$C_3H_6Cl_2 + CH_2Cl^+\{Cl_{11}^-\} \rightarrow C_3H_5^+\{Cl_{11}^-\} + CH_2Cl_2 + HCl \quad (2)$$

By this reaction, using dichlorobutane, the $C_4H_7^+$ cation has been obtained.[18] The completion of reaction 2 was monitored by measuring the absorption intensity of the formed gaseous CH_2Cl_2 and HCl. The $CH_2Cl^+\{Cl_{11}^-\}$ salt was prepared as described previously[23] according to eq 3

$$CH_2Cl_2 + H\{Cl_{11}\} \rightarrow CH_2Cl + \{Cl_{11}^-\} + HCl \quad (3)$$

After the completion of reaction 2, the absorption intensity of the released HCl reaches that of HCl formed during the preparation of the $CH_2Cl^+\{Cl_{11}^-\}$ salt when the molar ratio of $HCl/H\{Cl_{11}\}$ is 1.0 (eq 3). This finding confirms the mechanism of the reaction presented in eq 2. The IR spectrum of the resultant product belongs to the high-quality $C_3H_5^+\{Cl_{11}^-\}$ salt (Figure 3). If DCP vapors continue to be in contact with $C_3H_5^+\{Cl_{11}^-\}$ for more than 1 min, the spectrum of side products emerges. In this work, only salts of the carbocation $C_3H_5^+$ were studied; the products of its interaction with DCP will be a subject of a separate study.

The easiest way to obtain a large amount of the salt of the carbocation $C_3H_5^+$ is the direct interaction of liquid DCP with the $H\{Cl_{11}\}$ acid. When a small drop of DCP is added to the acid powder, the attenuated total reflectance (ATR) IR spectrum shows the formation of a salt of the $C_3H_5^+$ cation contaminated with the byproducts of its interaction with DCP. The intensity of the byproducts' spectrum depends on the quantity of added DCP. By repeating this experiment several times with different amounts of DCP injected, we were able to obtain a sample with a high-quality spectrum of $C_3H_5^+$ (Figure 4). It matches the spectra of the salts of $C_3H_5^+$ obtained in the IR cell reactor after an interaction of DCP vapors with the sublimed acid or the $CH_2Cl^+\{Cl_{11}^-\}$ salt.

To determine the structure of the carbocation, X-ray structural analysis was used. The pure $C_3H_5^+$ $\{Cl_{11}^-\}$ salt obtained by completing the reaction of DCP with $CH_2Cl^+\{Cl_{11}^-\}$ in a gas cell was dissolved in dichloromethane (DCM) and kept over hexane vapor. After a while, the crystals grew. X-ray structural analysis revealed that this is a $C_3H_5^+\{Cl_{11}^-\}$ salt with discrete cations and anions. Despite the rather large *R*-factor due to low-quality crystals (they are twins), the shape of the cation is clear-cut, making it possible

https://doi.org/10.1021/acsomega.1c01316
ACS Omega 2021, 6, 23691−23699

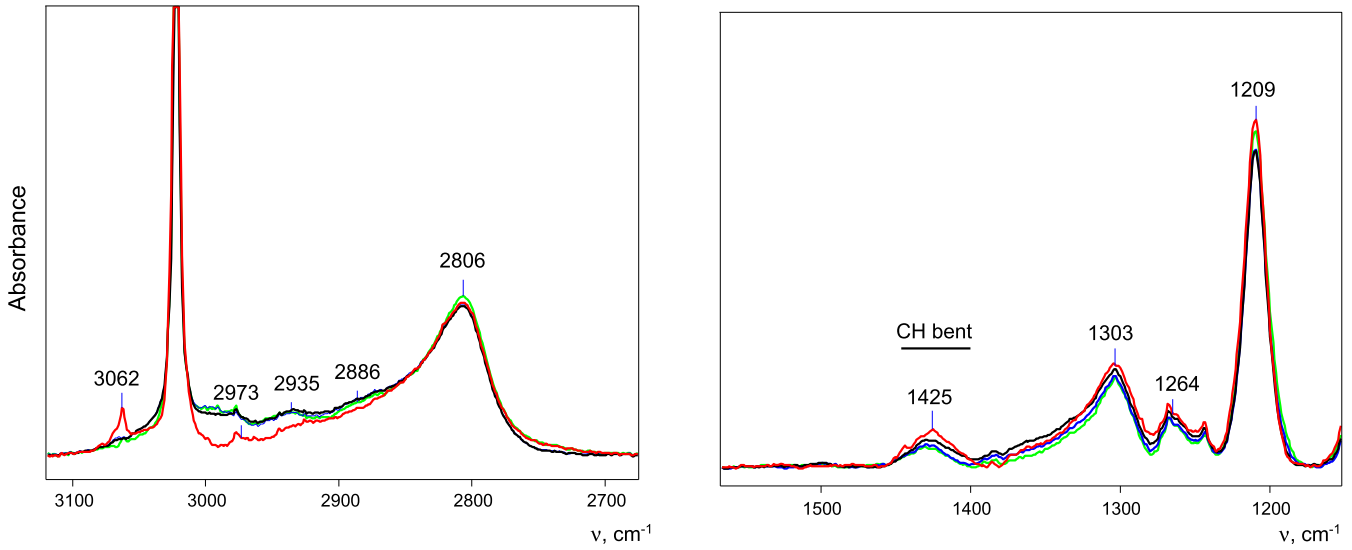

Figure 3. IR spectra of salt $C_3H_5^+\{Cl_{11}^-\}$, formed by the interaction of DCP with $CH_2Cl^+\{Cl_{11}^-\}$.

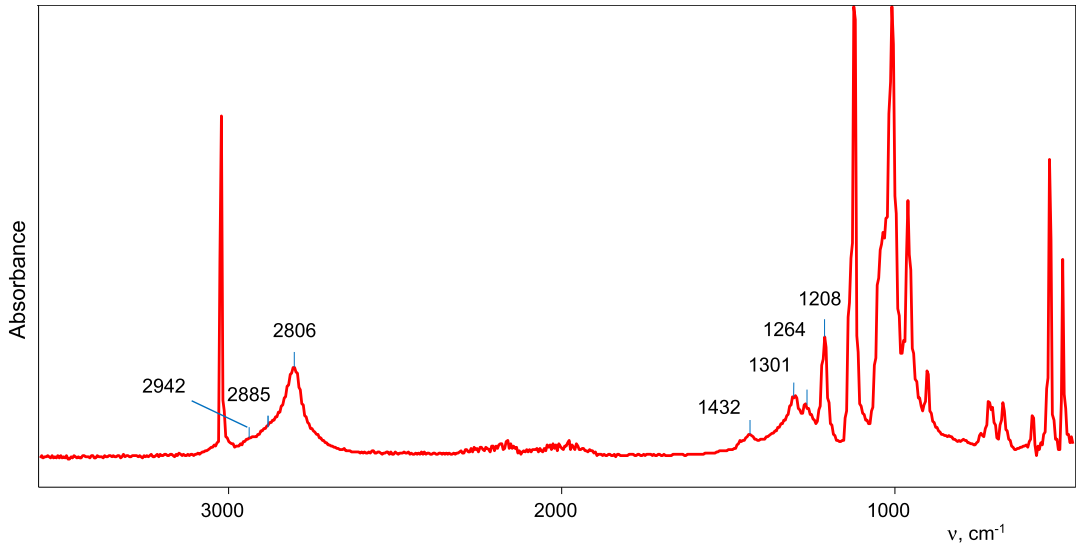

Figure 4. ATR IR spectrum (with ATR correction) of the amorphous $C_3H_5^+\{Cl_{11}^-\}$ salt. Some frequencies of the $C_3H_5^+$ cation are indicated; the other intense bands belong to the anion.

to determine its main structural features (Figure 5): it is an angular molecule with a central sp^2 carbon atom and one shortened CC bond close to a double one. Hereafter, we will refer to it as isomer **I**.

Crystals of the salt of another isomer of $C_3H_5^+$ were obtained as well. The salt $C_3H_5^+\{Cl_{11}^-\}$ obtained by the direct interaction of the acid with a small amount of DCP (its IR spectrum is given in Figure 4) was dissolved in *ortho*-dichlorobenzene and left over CCl_4 vapors for crystal growth.

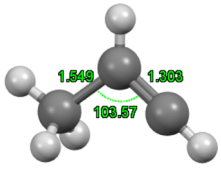

Figure 5. Structure of isomer **I** in the $C_3H_5^+\{Cl_{11}^-\}$ salt as determined by X-ray crystallography. The CC distances are given in Å, and the CCC angle are given in degrees.

After a while, a viscous dark-brown phase separated out. It was dissolved in DCM and left over hexane vapor. Crystals grew after 1−3 days. Their X-ray structure revealed that this is a $C_3H_5^+\{Cl_{11}^-\}$ salt with discrete cations and anions. Cations are linear, with the CCC angle of 180°, which means that the central C atom features sp hybridization, that is, we are dealing with the isomer $CH_3{-}C^+{=}CH_2$, which we designated as **II**. In the crystal lattice, the cations of this isomer are positioned in two orientations at an angle of 90° toward each other, which leads to different interactions with neighboring cations (Figure 6) and, as a consequence, to different distances between terminal carbon atoms, 1.513 and 1.432 Å. Thus, isomer **II** can be subdivided into two nonequivalent states: **IIa** and **IIb**. The longer isomer (1.513 Å) will be designated below as **IIa**, and the shorter one (1.432 Å) will be designated as **IIb**. The finding that crystallographic CC distances in both states, **IIa** and **IIb**, are aligned means that their visible structures are the result of the superposition of two oppositely oriented species, as shown in Scheme 1. Isomer **IIa** is in one crystallographic layer, and isomer **IIb** is in the other. **IIa** and **IIb** are arranged

https://doi.org/10.1021/acsomega.1c01316
ACS Omega 2021, 6, 23691−23699

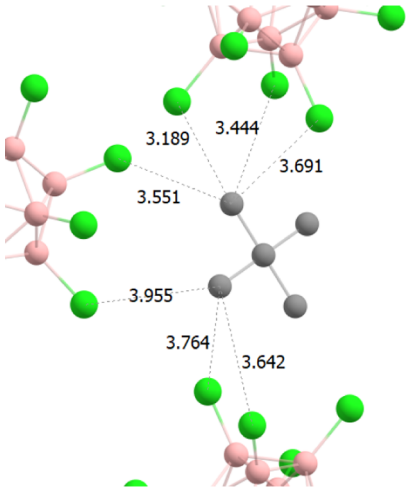

Figure 6. Structure of the $C_3H_5^+\{Cl_{11}^-\}$ salt containing isomer **II** in two orientations (at an angle of 90° toward each other), which are superimposed on each other (see Scheme 1). The shortest C···Cl distances (in Å) between the cation and anion are indicated.

relative to each other at an angle of 90°, and their crystallographic overlap looks like a cross (Scheme 1, Figure 6), in which the weight of the occupancy of position C1,4 is 1.0, whereas the weights of the occupancy of other positions, C3−C6, are 0.5.

3. DISCUSSION

IR spectra of three isomers of the $C_3H_5^+$ cation in its salts with the $\{Cl_{11}^-\}$ anion were registered, but crystal structures of only two of them (**I** and **II**) could be determined (Figures 5 and 6, Scheme 1).

The IR spectrum of angular isomer **I** contains intense bands of C═C and C−C stretching. Their frequencies actually match those of the $(CH_3)_2C{=}CH^+$ cation (Figure 7), in which the charge is localized on the $CH{=}CH^+$ group.[18] If one CH_3 group in the isobutylene$^+$ cation is replaced by an H atom to form **I**, then, the charge on $CH{=}CH^+$ can increase because the H atom is more electronegative than the CH_3 group. Nevertheless, this does not happen (the C═C stretching actually does not change), probably due to the participation of the CH_3 group of **I** in weak hyperconjugation with the p_z orbital of the central C atom (its CH stretches decrease to 2890 cm^{-1}), while the isobutylene$^+$ cation does not undergo hyperconjugative stabilization (Figure 7). In other words, a decrease in cation size from isobutylene$^+$ to propylene$^+$ leads to a decrease in the population of the $2p_z$ orbital of the central sp^2 C atom and to involvement of the CH_3 group in hyperconjugation that promotes the dispersion of the charge onto the H atoms of the CH_3 group without increasing positive-charge density on the $CH{=}CH^+$ moiety.

Cation **I** is located rather loosely in the cage of the crystal lattice formed by bulky anions and is engaged in a purely ionic interaction with them because the shortest C···Cl distances between the cation and the surrounding anions are 3.934 Å (Figure S2 in the Supporting Information), which exceeds the sum of van der Waals radii r_C and r_{Cl} (3.53 Å).[24] This observation indicates a uniform distribution of the positive charge over the cation.

Linear isomer **II** has two nonequivalent states, **IIa** and **IIb**, which, being differently oriented in the crystal lattice, interact differently with counterions. The shortest C···Cl distances between C atoms of the cation and Cl atoms of the anions in **IIa** are smaller (3.189 and 3.444 Å), while in **IIb**, they exceed (3.642 Å; Figure S3 in the Supporting Information) the sum of van der Waals radii r_C and r_{Cl} (3.53 Å). Therefore, isomer **IIa** strongly interacts with the surrounding anions through H-bonding, which lengthens its averaged CC bonds (1.513 Å) as compared with isomer **IIb** (1.432 Å). Therefore, isomers **IIa** and **IIb** should certainly differ in frequencies of C═C stretches, showing two νC═C bands in the IR spectra. Moreover, because each cation, **IIa** and **IIb**, has two opposite orientations (Scheme 1) in which they can be nonequivalent, the number of νC═C bands can reach three−four. In fact, the IR spectra show three bands of the C═C stretch at 1588, 1576, and 1564 cm^{-1} (Figure 8). Accordingly, in the frequency range of C−H stretch vibrations, three broad bands are observed—at 2897, 2854, and 2823 cm^{-1}—which are characteristics of CH_3 groups participating in hyperconjugation of different strengths. Therefore, we can say that at least three of the four differently oriented isomers **II** are nonequivalent, that is, each shows distinct charge dispersion over the cation.

The IR spectrum of the cation in the amorphous $C_3H_5^+\{Cl_{11}^-\}$ salt, arising when DCP interacts with the powdered acid, differs greatly from the spectra of isomers **I** and **II** (Figure 4) and belongs to another isomer, denoted as **III**. Its salt is a precursor for obtaining crystals containing isomers **I** and **II** but does not yield crystals of isomer **III** itself and therefore could not be characterized by X-ray crystallography. The main features of the IR spectrum of **III** (Figures 3 and 4) are low frequencies of CC and CH stretches, which almost match those of *i*-propyl$^+$ and *t*-butyl$^+$, $CH_3{-}C^+X{-}CH_3$ (where X = H or CH_3) or the charged moiety $-CH_2{-}C^+H{-}CH_2-$ in *cyclo*-pentyl$^+$ carbocations (Table 1). Their CH_3 or CH_2 groups take part in the hyperconjugation with the p_z orbital of the central sp^2 C atom, thereby decreasing the CH stretches and bringing the CC stretch vibrations closer to the values typical for one-and-a-half bond status. Such a good match of C−H and C−C stretches of **III** to those of saturated carbocations suggests that isomer **III** is a symmetric allyl cation $(CH_2CHCH_2)^+$. If it has the structure **IIIa** (Scheme 2), then, the charge should be more concentrated on the terminal CH_2 groups, thus reducing the probability of their involvement in hyperconjugation. If two CH_2 groups form a weak CC bond,

Scheme 1. Schematic Representation of Isomer II in Different Orientations in the Crystal Lattice

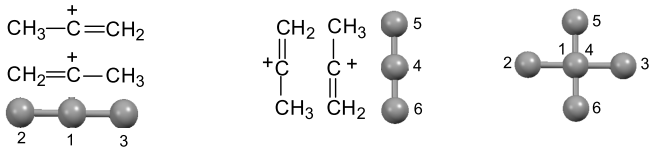

Isomer **IIa** Isomer **IIb** Crystallographic overlap of **IIa** and **IIb**

https://doi.org/10.1021/acsomega.1c01316
ACS Omega 2021, 6, 23691−23699

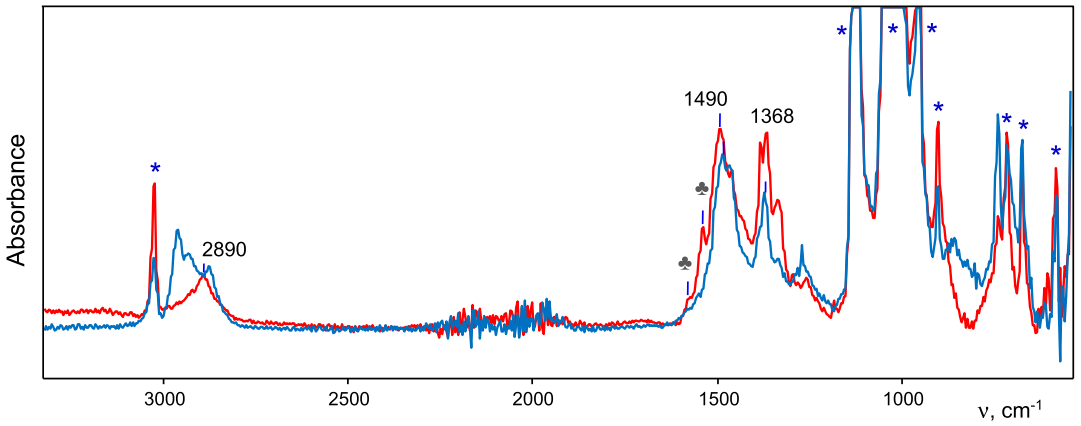

Figure 7. ATR IR spectra of crystalline salts with isomer I (red) or its analogue, butylene$^+$ cation $(CH_3)_2CH{=}CH^+$ (blue),[18] as analyzed by X-ray diffraction. The intense bands marked with asterisks belong to anion $CHB_{11}Cl_{11}^-$, and the weak bands at 1576 and 1537 cm^{-1} marked with black club suit belong to byproducts (for details see Figure S1 in the Supporting Information).

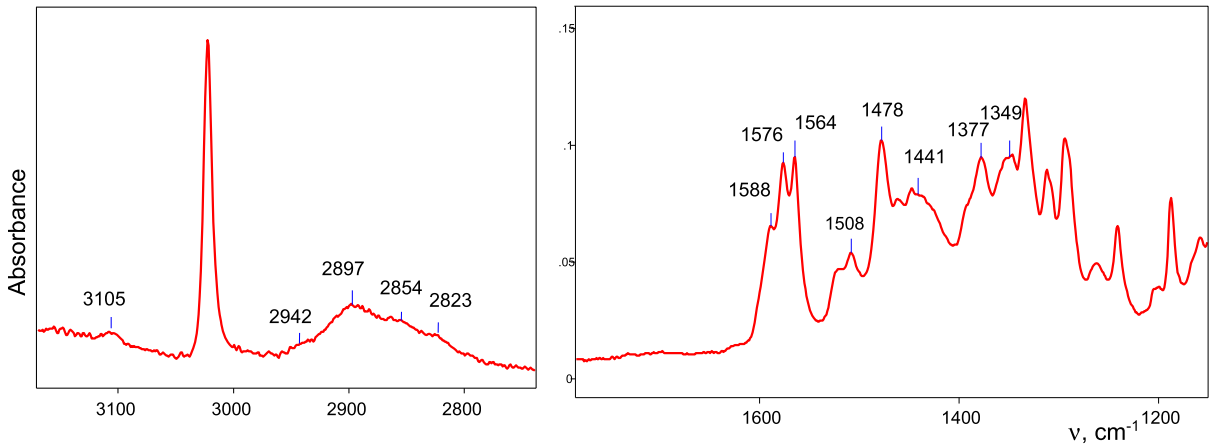

Figure 8. ATR IR spectrum of isomer **II** in crystalline salt $C_3H_5^+\{Cl_{11}^-\}$.

Table 1. Comparison of the Most Characteristic CH and CC Stretch Frequencies of Isomer III with Those of the Saturated Carbocations in the Salts with $\{Cl_{11}^-\}$ Ions

cation	C−H stretch[a]	CC stretches		refs
isomer **III**	2806	1303	1264	Present work
i-$C_3H_7^+$	2780	1256 broad		3
t-$C_4H_9^+$	2791	1289	1262	25
cyclo-pentyl$^+$	2780	1260 broad		3

[a]The most intense highly characteristic band of CH stretch vibration of the CH_3 or CH_2 group involved in hyperconjugation.

Scheme 2. Schematic Representation of Possible Structures of Isomer III

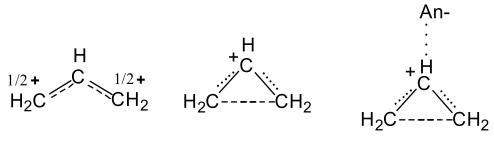

IIIa **IIIb′** **IIIb″**

converting the isomer to cyclic **IIIb′** (Scheme 2), then, the "+" charge will be more concentrated on the central C atom, and its p_z orbital may be empty enough to accept σ-electrons of CH_2 groups. Moreover, the orientation of their CH bonds will be optimal for the hyperconjugation with the $2p_z$ orbital. The similarity of frequencies of C−H stretches of **III** to those of saturated carbocations means that we are dealing with isomer **III** stabilized by stronger hyperconjugation than **I** and **II** are. The $(H_2)C{\cdots}C(H_2)$ bond in **IIIb′** should be weak because after the salt of **IIIb** is dissolved in DCM followed by crystallization, this bond breaks, giving rise to open-chain isomers **I** and **II**.

It is demonstrated below that upon optimization of structures **IIIa** and **IIIb′** (at the MP2 level), isomer **IIIb′** is transformed into **IIIa**, that is, it is unstable in vacuum. In the solid amorphous phase, **IIIb** can be stabilized by ion pairing, as seen in the salt of isobutylene, $C_4H_7^+\{Cl_{11}^-\}$:[18] the disordered anionic environment of the cation in the amorphous phase promotes a closer interaction of one of the anions with the most charged CH^+ group via H-bonding (Scheme 1). This situation increases intramolecular stabilization of the cation through the hyperconjugation effect.

Ionic pairing may also be responsible for the increased thermal stability of isomer **IIIb**. If a thin layer of the salt of **III** is quickly heated on the Si window of an evacuated IR cell to 100 °C, kept at this temperature for 5 min, and then quickly cooled down to room temperature, then, no changes are observed in the IR spectrum of the sample. Upon repeated heating of the sample under the same conditions to 120 °C, the intensity of the initial spectrum of isomer **III** decreases to 92%, and therefore, 8% of the isomer transitions to another

https://doi.org/10.1021/acsomega.1c01316
ACS Omega 2021, 6, 23691−23699

species. Next, after the sample is heated to 150 °C, 34.4% of the intensity of the **III** spectrum is retained, and spectrum intensity of the new products increases significantly.

Isomer **I** formally derives from neutral propene upon elimination of H^- from its $=CH_2$ group (Scheme 3). This event decreases electron density on the double C=C bond, and C=C stretch frequency should decrease. Indeed, the observed decrease in νC=C is (1652 − 1490) = 162 cm^{-1}.

Scheme 3. Illustration of the Formation of I from Propene

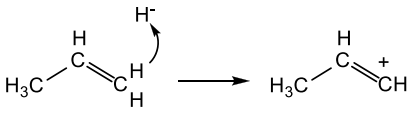

Rearrangement of the $-CH=CH^+$ group into the $-C^+=CH_2$ group, when **I** transitions to **II**, promotes a "+" charge shift to the central C atom, thereby somewhat enhancing the participation of the CH_3 group in hyperconjugation (its CH stretch decreases, Table 2). Better scattering of the positive charge onto the atoms of the CH_3-C moiety weakens its effect on the C=C bond, thus reducing the low-frequency shift of the C=C stretch relative to neutral propene to ∼76 cm^{-1} (recall that for **I**, this decrease is 162 cm^{-1}, Table 2).

Isomer **III** does not contain a double CC bond; therefore, the difference between its asymmetric CCC vibration and the C=C stretch of neutral butane is the greatest (∼350 cm^{-1}). Consequently, the frequencies of CC stretches are the best indicators for the identification of isomers **I**–**III** of the $C_3H_5^+$ cation (Table 2).

Our results are not consistent with the predictions of quantum chemical calculations for bare cations in vacuum. Geometry optimizations of isomers **I**–**III** (Scheme 4) and harmonic frequency calculations at the MP2 level of theory with the 6-311G++(d,p) basis set (Table S3 in the Supporting Information) yielded the following results.

Isomer **IIIa** is the most energetically favorable in vacuum. In comparison to it, the energies of **II** and **I** are higher by 12.5 and 25.1 kcal/mol, respectively. When isomer **IIIb** was optimized, the energy minimum was not reached because it is transformed into **IIIa**. In linear isomer **II**, the sum of two CC bond lengths (2.658 Å) is significantly less than experimentally determined values of 2.864 and 3.026 Å, thereby definitely indicating a strong influence of the environment. The optimized geometry of **I** differs most strongly from the experimental one. In fact, it represents an acetylene molecule, to which bridging CH_3^+ is attached, forming two long CC bonds of 1.695 and 1.873 Å, which are unheard of for hydrocarbon molecules. Optimization of isomers **I**, **II**, **IIa**, and **IIIb** at the B3LYP/6-311++G(d,p) level of theory predicts the stability of only two isomers, **II** and **IIIa**, while isomer **I** is converted to **II**, and **IIIb** is converted to **IIIa**. Thus, in the solid phase, the interaction of the cation with the anionic environment plays an extremely important role in the stabilization of cations by changing their energy state and electron density distribution. Therefore, it is not surprising that the calculated frequencies of such isomers also differ from the experimental ones. The greatest differences are seen in the frequencies of C=C stretches. For isomers **I** and **II**, they exceed those calculated for neutral propene by as much as 200 and 210 cm^{-1}, respectively, while experimental νC=C values are decreased by 162 cm^{-1} (**I**) and ∼76 cm^{-1} (**II**). This is a drastic mismatch, reaching 362 and 286 cm^{-1}. Indeed, the formation of the $C_3H_5^+$ cation upon elimination of H^- from the propene molecule lowers electron density on the bonding MO of the C=C bond, and its vibration frequency can only decrease, which is observed experimentally. By contrast, according to calculations, the C=C stretch frequency in this case should greatly increase with the shortening of the C=C bond, which means its strengthening. This is possible if the electron density decreases in the populated antibonding orbital. On the other hand, the C=C bond of propene does not contain such a populated orbital. Consequently, the results of calculations are unclear and cannot be used for a comparison with experimental data for cations I–III. A similar discrepancy between the experimental and calculated spectra has been reported for the isobutylene$^+$ cation.[18]

Direct examination of the allyl cation formation in a cryogenic superacid matrix (130 K) by IR spectroscopy has been performed by von R Schleyer et al.[17] The observed intense IR band at 1577–1581 cm^{-1}, which is closest to the calculated (CISD/6-31g**) asymmetric CCC vibration of isomer **IIIa**, was assigned to isomer **IIIa**, while it matches that of isomer **II** of the present work. On warming to 170 K, the allyl cation is converted to an undefined product with a band at 1547 cm^{-1}, perhaps a polymer. The assumption about the polymerization of the allyl cation at temperatures above 180 K

Table 2. Most Characteristic Frequencies of CH and CC Stretches of Isomers I–III and of the *i*-Butylene$^+$ Cation[a]

Isomer	CH stretch[b] exp.	C=C stretch Calc. (Δ[c])	Exp. (Δ[d])	C----C----C stretch asym. Calc. (Δ[c])	Exp. (Δ[d])
I  crystal	2890	1842 (200)	1490 (-162)	-	
II 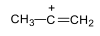 crystal	2987 2854 2823	1853 (210)	1588 1576 1564 (-64) (-76) (-88)	-	
III  amorphous	2806	-	-	1607 (-44)	1303 (-349)
i-butylene$^+$ 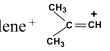 crystal	2960 2930 2874	1882 (217)	1485 (-175)	-	

[a]The difference between calculated (scaled by a factor of 0.9674) or experimental CC stretches and those of neutral propene or isobutene is given in parentheses. [b]The most intense C–H stretch vibration of the CH_3 or CH_2 groups; underlined frequencies belong to those groups that are involved in hyperconjugation. [c]A difference from the calculated C=C stretch for neutral propene (1643 cm^{-1}) or butene (1655 cm^{-1}). [d]A low-frequency shift relative to the experimental C=C stretch of neutral propene (1652 cm^{-1}) or butene (1660 cm^{-1}).

https://doi.org/10.1021/acsomega.1c01316
ACS Omega 2021, 6, 23691–23699

Scheme 4. Optimized Structures at the MP2 Level of Theory with the 6-311G++(d,p) Basis Set

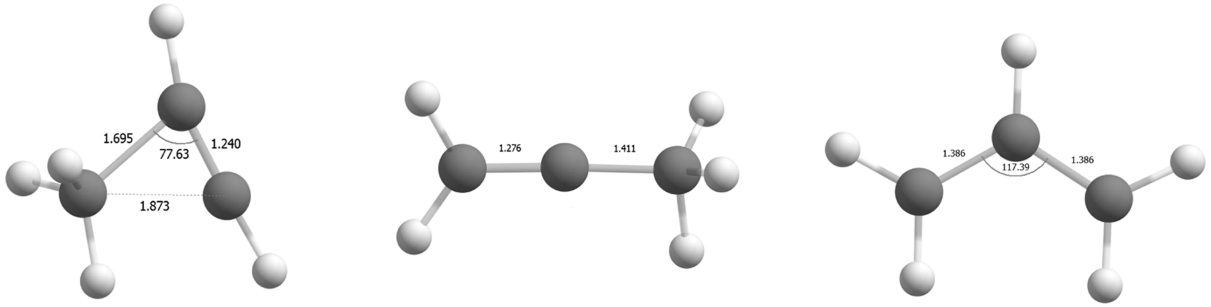

I **II** **IIIa**

cannot be correct because we found that all the identified isomers of $C_3H_5^+$ do not polymerize even at room temperature. The transition of the band near 1578 cm^{-1} to another one at 1547 cm^{-1} upon heating to 170 K and above can be caused by a change in the interaction of isomer **II** with the immediate environment. Given that the observed spectra contain many more peaks than are computed for the allyl cation, these authors[17] proposed that oligomerization or other side reactions must have occurred even at the low temperatures. By contrast, we found that oligomerization can occur only in the presence of an excess of the precursor that interacts with the formed allyl cation. One of the highly intense "extra" bands of the allyl cation observed at 170 K and shown in a figure in ref 17 has a frequency slightly lower than 1500 cm^{-1}, which is similar to the C═C stretch of isomer **I**. These authors did not show the frequency of this band because they did not classify it as an allyl cation, probably owing to its unexpectedly low frequency, which does not match any of the calculated CC stretch frequencies. Unfortunately, the CH stretches are not specified and discussed in that work. Thus, we can say that in a cryogenic superacidic matrix, the IR spectra of the allyl cation contain the bands of C═C stretches similar in frequency to those of isomers **II** and possibly **I** found in the present study.

There is an experimental study on the allyl cation, $C_3H_5^+$, tagged with either an N_2 or Ar molecule in vacuum by IR photodissociation spectroscopy.[15] Although we concluded that an IR spectroscopic comparison of allyl cations between solid and gas phases is inappropriate due to the strong influence of the environment, such a comparison is useful to make. The C═C stretches of two isomers $C_3H_5^+$ were detected at $1581_{N_2}/1585_{Ar}$ and $1877_{N_2}/1880_{Ar}$ cm^{-1}. The former is very close to the νC═C calculated for **IIIa** (1583 cm^{-1} after scaling by a factor of 0.955); this result allowed the authors to assign it to isomer **IIIa**, while it is close to the νC═C of isomer **II**, which we identified by X-ray crystallography. The latter spectrum with a frequency of the C═C stretch at $1877_{N_2}/1880_{Ar}$ cm^{-1} is close to that calculated for isomer **II**, thereby allowing assignment to isomer **II**. Unfortunately, a spectrum with $\nu C{=}C = 1877_{N_2}/1880_{Ar}$ cm^{-1} is different from any of the three possible isomers of $C_3H_5^+$ identified in the present work.

Bally et al. have generated the $C_3H_5^+$cation by ionization of the $C_3H_5^\bullet$ radical in an Ar matrix.[16] Its IR spectrum is in good agreement with that of gaseous $C_3H_5^+{\cdot}Ar(N_2)$,[15] and they also assigned it to isomer **IIIa** because of its good correlation with the calculated spectrum (for the frequency region below 1600 cm^{-1}). Nevertheless, its most characteristic strong band of the CC stretch at 1577 cm^{-1} matches one of the νC═C bands of the isomer **II** studied in the present work by X-ray crystallography.

It is possible that such a discrepancy between the results of the study of allyl cations in the gas phase according to the interpretation of IR spectra using quantum chemical calculations and solid-phase studies based on X-ray data is indeed due to the different distributions of electron density in cations **I**–**III** when they are isolated in vacuum versus cations **I**–**III** surrounded with anions in a solid phase. Nevertheless, the authors[15] left without an explanation the following important questions: Why does the experimental frequency of the C═C stretch at 1877/1880 cm^{-1}, assigned to isomer **II**, exceeds that of neutral propene by 228 cm^{-1}? (Which means that the emergence of the positive charge on the C═C bond causes a significant increase in the electron density on it, bringing it closer to a triple bond.) Why is the frequency at 1585 cm^{-1} (ref 15) or at 1577 cm^{-1} (ref 16)—assigned to the asymmetric CCC stretch of **IIIa**—close to stretch vibration of the C═C double bond of neutral propene?

4. CONCLUSIONS

The formation of all three possible isomers of the $C_3H_5^+$ cation in its solid carborane salts was demonstrated. The energetically most favorable symmetric allyl cation **III** forms in an amorphous phase and is stabilized by ion paring and strong hyperconjugation. The available experimental data indirectly point to its possible cyclization giving rise to a weak $(H_2)C{\cdots}C(H_2)$ bond. In the crystal lattice, isomer **III** is converted into identified isomers **I** and **II** with the disappearance of ion paring.

Linear isomer **II** is located in a loose cage of the crystal lattice and is oriented differently toward the anions. Due to the nonequivalent interactions with them, it manifests three distinct C═C stretches. This finding indicates that the distribution of electron density along its CC bonds is very sensitive to the influence of the environment. Identical frequencies of the C═C stretch of isomer **II** have been registered for the allyl cation in a cryogenic superacidic matrix (where it was attributed to the isomer **III**).[17]

The existence of angular isomer **I** (the least thermodynamically stable in vacuum) in crystalline salts was proved by X-ray structural analysis. It is an analogue of isobutylene carbocation $(CH_3)_2C{=}CH^+$, which should also be the least stable in vacuum among all possible isomers of the butene cation, but has been proven to exist in carborane salts by X-ray crystallography.[18] IR spectra of isomer **I** and carbocation $(CH_3)_2C{=}CH^+$ are very similar too. IR spectra of isolated $C_3H_5^+$ cations in a cryogenic SbF_5 matrix[17] apparently contain

https://doi.org/10.1021/acsomega.1c01316
ACS Omega 2021, 6, 23691−23699

the characteristic C=C stretch vibrations of isomer **I**. Isomers **I** and **II** are stabilized in the crystal lattice by uniform ionic interactions with neighboring anions. Cation **II** shoes additional intramolecular stabilization by weak hyperconjugation. The influence of the environment should cause a noticeable difference between the IR spectra of the $C_3H_7^+$ isomers in the solid phase and those in the gas phase. These differences were found and require further study.

The discovered discrepancies between the experimental data and the predictions of quantum chemical calculations can be illustrated by means of the following example. The observed significantly lower frequencies of the C=C stretch of isomers **I** and **II** relative to neutral propene correspond to those expected when H^- is subtracted from the C_3H_6 molecule affording an electron-deficient $C_3H_7^+$ cation. However, quantum chemical calculations predict that in this case, electron density on the C=C bond of the cation should increase. This contradiction is yet to be resolved.

5. EXPERIMENTAL SECTION

All sample handling was carried out in an inert atmosphere (H_2O, O_2 < 1 ppm) in a glovebox. The carborane acid, $H\{Cl_{11}\}$, was prepared as described previously.[26] It was purified by sublimation at 150−160 °C under a pressure of 10^{-5} Torr on cold Si windows in a specially designed IR cell reactor, whose detailed description is given in ref 18. The formed thin translucent layer yielded an intense IR spectrum. The $C_3H_7^+\{Cl_{11}^-\}$ salt was obtained by injection of gaseous DCP under anaerobic conditions into the IR cell reactor containing the acid. To determine the molar ratio of released HCl to reacted $H\{Cl_{11}\}$, absorption intensity of the formed gaseous HCl was measured at a frequency of 2821 cm^{-1} (I_{2821}), and using the calibration plot of I_{2821} versus HCl content (in millimoles) for a given IR cell, it is converted to millimoles. The amount of the reacted acid was determined by treating the final reaction product with a 0.1 M NaOH solution, followed by back titration with a standard 0.1 M HCl solution. The observed molar ratio of HCl/reacted acid is close to 2, which corresponds to the overall reaction described by eq 1. The second way to obtain $C_3H_7^+\{Cl_{11}^-\}$ by means of the $CH_2Cl^+\{Cl_{11}^-\}$ salt is described in the main text.

DCP from Toronto Research Chemicals Inc. was used without further purification.

X-ray diffraction data were obtained on a Bruker Kappa Apex II CCD diffractometer using φ and ω scans of narrow (0.5°) frames with Mo Kα radiation (λ = 0.71073 Å) and a graphite monochromator. The structures were solved by direct methods by means of the SHELX-97 software suite[27] and were refined by the full-matrix least-square method against all F^2 in anisotropic approximation in SHELXL-2014/7.[28] Absorption corrections were applied by the empirical multiscan method in SADABS software.[29] Hydrogen atoms' positions were calculated with the riding model. Crystallographic data and details of the X-ray diffraction experiment are listed in Table S1 in the Supporting Information. CCDC 2063010 and 2063011 contain the supplementary crystallographic data for this paper. These data can be obtained free of charge via http://www.ccdc.cam.ac.uk/cgi-bin/catreq.cgi or from the Cambridge Crystallographic Data Centre, 12 Union Road, Cambridge CB2 1EZ, UK; fax: (+44) 1223 336 033; email: deposit@ccdc.cam.ac.uk.

The high *R*-factor for the salt of the $CH_3-CH=CH^+$ cation is explained by the bad quality of the crystals obtained. They are twins, and we failed to obtain crystals of the best quality. The structure was refined as 0.85:0.15 2-component twins. The structure of the salt of isomer $CH_3-C^+=CH_2$ is formed by crystallographically independent 1/2 part of the molecules of the anion and cation. The cation is located at the center of symmetry and is disordered at two positions.

The crystal structures were analyzed for short contacts between nonbonded atoms using PLATON[30] and MERCURY programs.[31]

DFT calculations were performed at the B3LYP/6-311G++(d,p) level plus the D3 dispersion correction energy term[32] with an ultrafine integration grid within the framework of the Gaussian'09 package. MP2 calculations were performed with the same 6-311G++(d,p) basis set with an ultrafine integration grid within the framework of the Gaussian 09 package.[33] To compare calculated and experimental vibrational frequencies, the calculated harmonic frequencies were scaled by a factor of 0.9674, as recommended by Kesharwani et al.[34]

■ ASSOCIATED CONTENT

Supporting Information

The Supporting Information is available free of charge at https://pubs.acs.org/doi/10.1021/acsomega.1c01316.

Details of X-ray data, additional IR spectra, and calculated frequencies for propene and $C_3H_7^+$ isomers (PDF)

■ AUTHOR INFORMATION

Corresponding Author

Evgenii S. Stoyanov − *N.N. Vorozhtsov Institute of Organic Chemistry, Siberian Branch of Russian Academy of Sciences, Novosibirsk 630090, Russia;* orcid.org/0000-0001-6596-9590; Email: evgenii@nioch.nsc.ru

Authors

Irina Yu. Bagryanskaya − *N.N. Vorozhtsov Institute of Organic Chemistry, Siberian Branch of Russian Academy of Sciences, Novosibirsk 630090, Russia*

Irina V. Stoyanova − *N.N. Vorozhtsov Institute of Organic Chemistry, Siberian Branch of Russian Academy of Sciences, Novosibirsk 630090, Russia*

Complete contact information is available at: https://pubs.acs.org/10.1021/acsomega.1c01316

Notes

The authors declare no competing financial interest.

■ ACKNOWLEDGMENTS

This work was supported by grant # 16-13-10151 from the Russian Science Foundation. The authors thank Viktor Yu. Kovalskii for performing the quantum chemical calculations. The English language was corrected and certified by shevchuk-editing.com.

■ REFERENCES

(1) *Stable Carbocation Chemistry*; Prakash, G. K. S., Schleyer, P. v. R., Eds.; John Wiley & Sons: New York, 1997.

(2) *Carbocation Chemistry*; Olah, G. A., Prakash, G. K. S., Eds.; John Wiley & Sons: Hoboken, NJ, 2004.

(3) Stoyanov, E. S.; Nizovtsev, A. S. Stabilization of carbocations CH_3^+, $C_2H_5^+$, i-$C_3H_7^+$, tert-Bu^+, and cyclo-pentyl$^+$ in solid phases: experimental data versus calculations. *Phys. Chem. Chem. Phys.* **2017**, *19*, 7270−7279.

(4) Hanack, M. Mechanistic and preparative aspects of vinyl cation chemistry. *Angew. Chem., Int. Ed.* **1978**, *17*, 333−341.
(5) Radom, L.; Hariharan, P. C.; Pople, J. A.; Schleyer, P. V. R. Molecular orbital theory of the electronic structure of organic compounds. XIX. Geometries and energies of C_3H_5 cations. Energy relations among allyl, vinyl, and cyclopropyl cations. *J. Am. Chem. Soc.* **1973**, *95*, 6531−6544.
(6) Stang, P. J.; Rappoport, Z. *Dicoordinated Carbocations*; Wiley, 1997.
(7) Müller, T.; Juhasz, M.; Reed, C. A. The X-ray structure of a vinyl cation. *Angew. Chem., Int. Ed.* **2004**, *43*, 1543−1546.
(8) Hinkle, R. J.; McNeil, A. J.; Thomas, Q. A.; Andrews, M. N. Primary Vinyl Cations in Solution: Kinetics and Products of *β*, *β*-Disubstituted Alkenyl(aryl)iodonium Triflate Fragmentations. *J. Am. Chem. Soc.* **1999**, *121*, 7437−7438.
(9) *Vinyl Cations*; Stang, P. J., Rappaport, Z., Hanack, M., Subramanian, L. R., Eds.; Academic Press: San Diego, 1979.
(10) Siehl, H.-U.; Müller, T.; Gauss, J. NMR Spectroscopic and quantum chemical characterization of the (E)− and (Z)− isomers of the penta-1,3-dienyl-2-cation. *J. Phys. Org. Chem.* **2003**, *16*, 577−581.
(11) Rablen, P. R.; Perry-Freer, N. A. How the arrangement of alkyl substituents affects the stability of delocalized carbocations. *J. Org. Chem.* **2018**, *83*, 4024−4033.
(12) Cunje, A.; Rodriqyez, C. F.; Lien, M. H.; Hopkinson, A. C. The $C_4H_5^+$ Potential Energy Surface. Structure, Relative Energies, and Enthalpies of Formation of Isomers of $C_4H_5^+$. *J. Org. Chem.* **1996**, *61*, 5212−5220.
(13) Duncan, M. A. Infrared laser spectroscopy of mass-selected carbocations. *J. Phys. Chem. A* **2012**, *116*, 11477−11491.
(14) Ricks, A. M.; Douberly, G. E.; Schleyer, P. v. R.; Duncan, M. A. Communications: Infrared spectroscopy of gas phase $C_3H_3^+$ ions: The cyclopropenyl and propargyl cations. *J. Chem. Phys.* **2010**, *132*, 051101.
(15) Douberly, G. E.; Ricks, A. M.; Schleyer, P. v. R.; Duncan, M. A. Infrared spectroscopy of gas phase $C_3H_5^+$: The allyl and 2-propenyl cations. *J. Chem. Phys.* **2008**, *128*, 021102.
(16) Mišić, V.; Piech, K.; Bally, T. Carbocations generated under stable conditions by ionization of matrix-isolated radicals: The allyl and benzyl cations. *J. Am. Chem. Soc.* **2013**, *135*, 8625−8631.
(17) Buzek, P.; von R Schleyer, P.; Vančik, H.; Mihalic, Z.; Gauss, J. Generation of the parent allyl cation in a superacid cryogenic matrix. *Angew. Chem., Int. Ed.* **1994**, *33*, 448−451.
(18) Stoyanov, E. S.; Bagryanskaya, I. Y.; Stoyanova, I. V. The Unsaturated Vinyl-type Isobutylene Carbocation in its Carborane Salts. *ACS Omega* **2021**, *6*, 15834.
(19) Mayr, H.; Lang, G.; Ofial, A. R. Reactions of carbocations with unsaturated hydrocarbons: Electrophilic alkylation or hydride abstraction? *J. Am. Chem. Soc.* **2002**, *124*, 4076−4083.
(20) Stoyanov, E. S.; Stoyanova, I. V. The Mechanism of High Reactivity of Benzyl Carbocation, $C_6H_5CH_2^+$, during Interaction with Benzene. *ChemistrySelect* **2020**, *5*, 9277−9280.
(21) Reed, C. A. Carborane acids. New "strong yet gentle" acids for organic and inorganic chemistry. *Chem. Commun.* **2005**, 1669−1677.
(22) Stoyanov, E. S.; Hoffmann, S. P.; Juhasz, M.; Reed, C. A. The Structure of the Strongest Brønsted Acid: The Carborane Acid $H(CHB_{11}Cl_{11})$. *J. Am. Chem. Soc.* **2006**, *128*, 3160−3161.
(23) Stoyanov, E. S. The salts of chloronium ions R−Cl^+−R (R= CH_3 or CH_2Cl): formation, thermal stability, and interaction with chloromethanes. *Phys. Chem. Chem. Phys.* **2016**, *18*, 12896−12904.
(24) Rowland, R. S.; Taylor, R. Intermolecular nonbonded contact distances in organic crystal structures: Comparison with distances expected from van der Waals radii. *J. Phys. Chem.* **1996**, *100*, 7384−7391.
(25) Stoyanov, E. S.; Gomes, G. d. P. tert-Butyl Carbocation in Condensed Phases: Stabilization via Hyperconjugation, Polarization, and Hydrogen Bonding. *J. Phys. Chem. A* **2015**, *119*, 8619−8629.
(26) Juhasz, M.; Hoffmann, S.; Stoyanov, E.; Kim, K.-C.; Reed, C. A. The strongest isolable acid. *Angew. Chem., Int. Ed.* **2004**, *43*, 5352−5355.
(27) Sheldrick, G. M. *SHELX-97, Programs for Crystal Structure Analysis (Release 97-2)*; University of Göttingen: Germany, 1997.
(28) Sheldrick, G. M. Crystal structure refinement with SHELXL. *Acta Crystallogr., Sect. C: Struct. Chem.* **2015**, *71*, 3−8.
(29) Sheldrick, G. M. *SADABS*, v. 2008-1; Bruker AXS: Madison, WI, USA, 2008.
(30) (a) Spek, A. L. *PLATON, A Multipurpose Crystallographic Tool* (Version 10M); Utrecht University: Utrecht, The Netherlands, 2003; (b) Spek, A. L. Single-crystal structure validation with the program PLATON. *J. Appl. Crystallogr.* **2003**, *36*, 7−13.
(31) Macrae, C. F.; Edgington, P. R.; McCabe, P.; Pidcock, E.; Shields, G. P.; Taylor, R.; Towler, M.; van de Streek, J. Mercury: visualization and analysis of crystal structures. *J. Appl. Crystallogr.* **2006**, *39*, 453−457.
(32) Grimme, S.; Antony, J.; Ehrlich, S.; Krieg, H. A consistent and accurate ab initio parametrization of density functional dispersion correction (DFT-D) for the 94 elements H-Pu. *J. Chem. Phys.* **2010**, *132*, 154104.
(33) Frisch, M. J.; Trucks, G. W.; Schlegel, H. B.; Scuseria, G. E.; Robb, M. A.; Cheeseman, J. R.; Scalmani, G.; Barone, V.; Petersson, G. A.; Nakatsuji, H.; et al., *Gaussian 09*, Revision D.01; Gaussian, Inc.: Wallingford CT, 2016.
(34) Kesharwani, M. K.; Brauer, B.; Martin, J. M. L. Frequency and Zero-Point Vibrational Energy Scale Factors for Double-Hybrid Density Functionals (and Other Selected Methods): Can Anharmonic Force Fields Be Avoided? *J. Phys. Chem. A* **2015**, *119*, 1701−1714.

https://doi.org/10.1021/acsomega.1c01316
ACS Omega 2021, 6, 23691−23699